Nanoscale Res Lett (2010) 5:649–653
DOI 10.1007/s11671-010-9529-x

NANO EXPRESS

Carbon-Coated SnO_2 Nanorod Array for Lithium-Ion Battery Anode Material

Xiaoxu Ji · Xintang Huang · Jinping Liu · Jian Jiang · Xin Li · Ruimin Ding · Yingying Hu · Fei Wu · Qiang Li

Received: 16 November 2009 / Accepted: 5 January 2010 / Published online: 21 January 2010

Abstract Carbon-coated SnO_2 nanorod array directly grown on the substrate has been prepared by a two-step hydrothermal method for anode material of lithium-ion batteries (LIBs). The structural, morphological and electrochemical properties were investigated by means of X-ray diffraction (XRD), scanning electron microscopy (SEM), transmission electron microscopy (TEM) and electrochemical measurement. When used as anodes for LIBs with high current density, as-obtained array reveals excellent cycling stability and rate capability. This straightforward approach can be extended to the synthesis of other carbon-coated metal oxides for application of LIBs.

Keywords Carbon-coated SnO_2 nanorod array · Hydrothermal method · LIBs · Anode material · Array architecture

Introduction

Rechargeable lithium-ion batteries (LIBs), as a dominant power source for portable electronic devices, have attracted much attention in the scientific and industrial fields [1]. The present configuration of a lithium-ion battery involves a graphite anode, a cathode ($LiCoO_2$) and a liquid organic-solution electrolyte [2]. Numerous efforts have been made to develop useful alternative materials or design new structures of electrode to meet the demand for LIBs with high energy density, excellent cycling performance and environmental compatibility [3–12].

As an important cost-effective wide band *n*-type semiconductor, tin oxide (SnO_2) has been widely applied in gas sensors, dye sensitized solar cells, transparent conducting coatings for glasses and electrodes. Besides, significantly believed to be potential building blocks for anode material of LIBs with its high theoretical specific capacity (718 mAh g^{-1}) when compared to graphite (372 mAh g^{-1}), nano-sized SnO_2 has been intensively investigated for the last decades [13]. However, the biggest bottleneck nowadays for future practical applications of SnO_2 as an applicable active electrode material is that large volume expansion/contraction ($\sim$300%) during repeated charge–discharge processes result in the pulverization of materials, this leads to the electrical disconnection between the anode materials and the current collector, severely decreasing the cycling ability of electrodes [14, 15].

One-dimensional (1D) nanomaterials, such as nanowires and nanorods, have become the focus of intensive research because of their unique properties recently. So much attention has been paid on the fabrication of 1D nanomaterials as anodes for LIBs owing to their large surface-to-volume ratio and relatively short diffusion length, which is regarded to fundamentally update the electrochemical kinetic properties [16–18]. Typically, aligned nanowires/nanorods arrays of SnO_2 have been demonstrated to be capable of providing more channels for efficient electron transportation than particle-based electrodes [19–21]. However, anodes of 1D nanostructure arrays still suffer from the fatal capacity decay. Therefore, optimizing the SnO_2-based materials with high performance is quite urgent. Up to date, some metal oxides and carbon nanocomposites have been reported with both high capacity and capacity retention when employed as anode materials

X. Ji · X. Huang (✉) · J. Liu · J. Jiang · X. Li · R. Ding · Y. Hu · F. Wu · Q. Li
Department of Physics, Central China Normal University, 430079 Wuhan, Hubei, People's Republic of China
e-mail: Volitation2009@163.com; xthuang@phy.ccnu.edu.cn

[7, 22–24], but well-designed SnO_2 nanoarrays coated with carbon have not been reported to date.

In this study, directly grown carbon-coated SnO_2 nanorod array on conducting bulk Fe–Co–Ni alloy substrate (atomic ratio of Fe:Co:Ni = 52.23:18.07:29.70) was made by a controllable hydrothermal method. Different from the traditional tedious technology of fabricating electrochemical electrodes, active materials have been directly grown on the electrode surface successfully. The robust firmness of oxide/substrate interaction ensures both the excellent electrical contact between active materials and the current collector and superior strain accommodation during preparation. Both the electrochemical advantages of array structure on conductive substrate and the electroactivity of carbon enhance the electrochemical performances of the novel array nanostructure. This new electrode is found to show high rate capability and long cycle life. To our knowledge, this is the first report on the application of carbon-coated SnO_2 nanorod array electrode in LIBs. This new nanostructure has been demonstrated to be an ideal electrode as anode of LIBs.

Experimental

Synthesis of Carbon-Coated SnO_2 Nanorod Arrays

In a typical synthesis, 2 mmol $SnCl_4{\cdot}5H_2O$ and 35 mmol NaOH were dissolved in a mixture of distilled water and ethanol to form a transparent solution. The solution was transferred into a Teflon-lined autoclave (a piece of an ethanol/water washed Fe–Co–Ni alloy substrate was placed in the autoclave). The autoclave was placed in an electric oven at 180°C for 24 h before it was cooled down to room temperature. After the reaction, the substrate was washed with distilled water and dried in a vacuum oven at 60°C for 6 h. Then, 1.2 mmol of glucose was dissolved in the mixture of distilled water and ethanol to form a transparent solution. A piece of as-obtained SnO_2 nanorod arrays on the conductive substrate was placed against the wall of the autoclave. Then, the mixed solution as mentioned previously was transferred to a 50-ml Teflon autoclave, which was then heated in an electric oven at 180°C for 18 h. After cooling down in air, the as-prepared product was washed with distilled water and dried in a vacuum oven at 100°C for 3 h. Hereafter, the substrate was carbonized at 450°C for 3 h under nitrogen flow to obtain carbon-coated SnO_2 arrays.

Characterization

The morphology of the as-prepared product was characterized by field-emission scanning electron microscopy (FESEM, JEOL, JSM-6700F). The sample was analyzed by X-ray diffractometer (XRD, Y-2000) with Cu Kα radiation ($\lambda = 1.5418$ Å) at a scan rate of $0.04°s^{-1}$. Transmission electron microscopy (TEM) observations were carried out on a JEOL JEM-2010 instrument.

Electrochemical Measurements

Electrochemical cells were assembled in an argon-filled glovebox using the as-obtained SnO_2 and carbon-coated SnO_2 nanorod array on alloy as anode material, respectively, and lithium foil directly served as the counter/reference electrode. As electrolyte, 1 M solution of $LiPF_6$ in ethylene carbonate (EC) and diethyl carbonate (DEC) (1:1 by volume) was employed. The charge–discharge cycling was performed by using a multichannel battery tester (model SCN, Bitrode, USA).

Results and Discussions

Morphology and Structure of Obtained Products

Throughout a complex polymerization of glucose at 180°C in the autoclave, scalable pencil-like SnO_2 nanorod arrays employed as the templates were initially coated by organic carbonaceous layers on their outer surface. As could be obviously observed from naked eyes, the sample turned from gray to brown, indicating that desired organic carbonaceous layers on SnO_2 nanorods were formed successfully [25]. As reported in the literatures, glucose-derived carbon precursor (PS) can be readily integrated onto nanostructure in solution and furthermore carbonized at a temperature as low as 400°C, while tin oxide could be carbothermally reduced to metallic tin by carbon only if the temperature reaches 600°C [22]. Accordingly, in this work, the overall carbonization process is finally determined at 450°C to avoid the destruction of SnO_2 nanorod arrays. After heat-treatment at 450°C for 3 h under nitrogen atmosphere, the sample becomes black, indicating the existing carbon layer.

Figure 1a shows the schematic diagram of the preparation procedures for the carbon-coated SnO_2 nanorod arrays. As manifested in Fig. 1b, the typical XRD pattern of the sample is displayed. Clearly except for the peaks originating from the alloy substrate, all the peaks are arising from the rutile structured SnO_2 (JCPDS No. 41-1445). The strongest peak is (101), revealing that individual SnO_2 nanostructures are crystallized along the *c*-axis grown on the substrate. Representative SEM image of as-obtained product is observed in Fig. 1c. The inset in Fig. 1c presents the cross-sectional image of the as-obtained product. As can be seen, the nanorods are also proved to grown on the substrate, with a typical mean sharp tip <100 nm and a

length of >400 nm, respectively. In addition, the amorphous carbon layer can be observed as well (indicated by black arrow).

The ordering of carbon layer is examined by the Raman spectrum analysis in Fig. 2a, which shows two strong peaks located at 1,379 cm^{-1} (D-band) and 1,585 cm^{-1} (G-band), confirming the presence and partial graphitization of carbon [26]. The decoration of carbon on the surface of individual SnO_2 nanorod is further investigated by TEM in Fig. 2b, from which a very thin carbon layer is markedly observed (indicated by black arrow). The average thickness of carbon layer is $\sim$6 nm. In addition, the single nanorod is coated by amorphous carbon with a uniform thickness.

Electrochemical Activities

To study the potential electrochemical application of as-obtained samples, we have investigated the Li storage properties of carbon-coated SnO_2 nanorod array on the alloy substrate, which serves as the working electrode directly. Herein Li foil serves as the counter electrode. As reported, the electrochemical reaction mechanism of Li with SnO_2 can be described in Eqs. 1 and 2.

$$SnO_2 + 4Li^+ + 4e^- \rightarrow Sn + 2Li_2O \quad (1)$$

$$xLi^+ + xe^- + Sn \leftrightarrow Li_xSn \ (0 \leqq x \leqq 4.4) \quad (2)$$

Recently, well-designed structures of SnO_2 electrodes have been demonstrated to improve the cycling capability, but their electrochemical performance at high current density was rarely investigated. Titirici et al. demonstrated that mesoporous SnO_2 microspheres via assembled nanoparticles could deliver reversible capacities of 370 and 200 mAh g^{-1} at a rate of 1 ($\sim$1.28 C) and 2 A g^{-1} ($\sim$2.56 C), respectively [27]. In this work, we investigated the electrochemical properties of as-obtained electrode on the high current density because it is important for the practical application of battery such as electric vehicles and portable powers. The assembled cell was cycled between 0.005 and 2.5 V at room temperature with a high current density of 500 mA g^{-1}. As expected, we found enhanced electrochemical result of carbon-coated SnO_2 nanorod array. As can be seen, carbon-coated SnO_2 array presented a higher reversible capacity and better cyclic retention up to the fiftieth cycle from Fig. 3. The coulombic efficiency for the first cycle is 58.2%, which is higher than many corresponding reports. The initial irreversible loss is

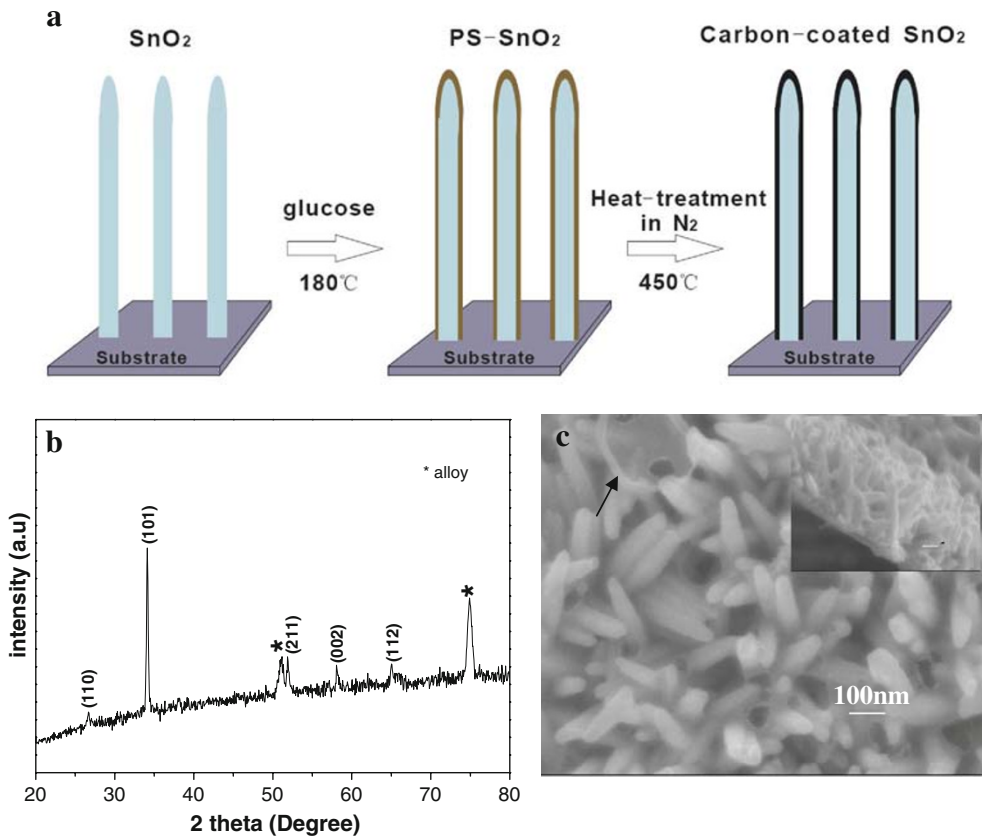

Fig. 1 **a** Schematic diagram of as-obtained carbon-coated SnO_2 nanorod array and **b** XRD of the as-obtained product on alloy substrate; **c** SEM image of array. *Inset* is the cross-sectional SEM image of array; the *black arrow* indicates the present of carbon layer

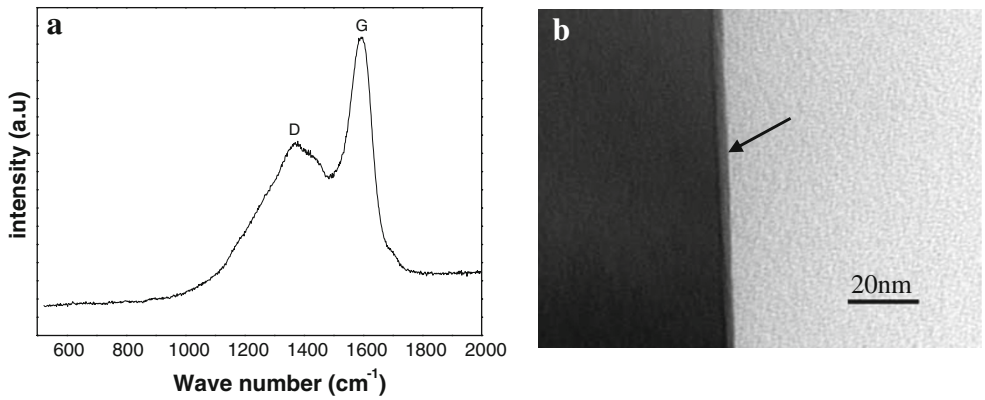

Fig. 2 **a** Raman spectrum of the carbon-coated nanorod array and **b** TEM image of an individual carbon-coated SnO_2 nanorod. The *black arrow* indicates the present of carbon layer

ascribed to the Li_2O phase electrochemically inactive and non-conductive, irreversible reduction of SnO_2 to Sn as described in Eq. 1, and decomposition of electrolyte to form a protective film on the electrode surface [25].

To demonstrate the advantages of carbon-coated array electrode, anode of pristine SnO_2 nanorod array and carbon-coated SnO_2 nanorod array were tested separately. Figure 3 displays the result of cycling performance of pristine SnO_2 array and carbon-coated SnO_2 array (capacity retention vs cycle number) at 500 mA g^{-1}. It is important to note that the capacity of carbon-coated SnO_2 array of around 585 mAh g^{-1} can be retained after 50 cycles, which is higher than the theoretical capacity of graphite (372 mAh g^{-1}). However, the capacity of pristine SnO_2 is only 320 mAh g^{-1} after 50 cycles, the excellent cycling performance of which could arise from good elasticity of carbon layer to accommodate the strain of volume change during cycling and improve the conductivity of this material. In the case of pristine SnO_2 nanorod array, a large volume expansion occurs during the cycling, leading to the pulverization of the electrode. To further demonstrate the advantages of carbon-coated SnO_2 array electrode, we investigated the cyclability at different high current densities. Figure 4 shows the discharge capacity versus cycle number. The cell reveals good cyclability at 1,500 mA g^{-1}, with capacity of 460 mAh g^{-1} after 50 cycles, which is about 23% higher than the theoretical capacity of graphite (372 mAh g^{-1}). Even at a high current density of 3,000 mA g^{-1}, the capacity of the electrode still retains 320 mAh g^{-1}, which is close to graphite capacity. With uniformly coated carbon, electrons can easily reach any positions where Li^+-ion intercalation takes place. This feature is particularly helpful when the battery is cycled at a high current density.

Conclusions

In summary, a new approach has been designed to prepare carbon-coated SnO_2 nanorod array directly grown on metal substrate. The as-made electrodes of carbon-coated nanorods have shown good performances, which has excellent capacity retention (585 mAh g^{-1} after 50 cycles at 500 mA g^{-1}) and cyclability (stable 320 mAh g^{-1} at 3,000 mA g^{-1}). The array grown directly on current collector substrate provides good electronic transportation.

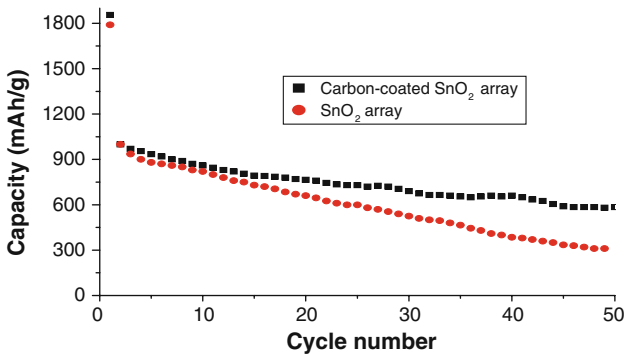

Fig. 3 Cycling performance of carbon-coated SnO_2 array and pristine SnO_2 array at a current density of 500 mA g^{-1}

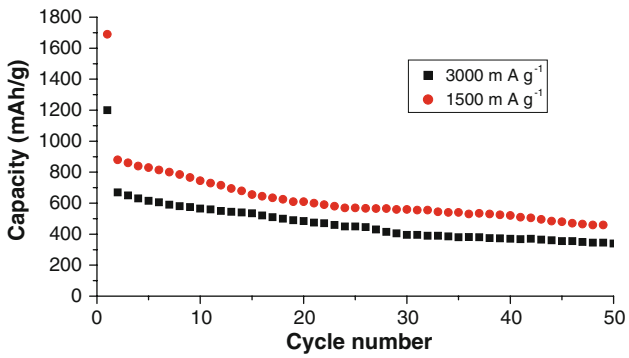

Fig. 4 Cycling performance of carbon-coated SnO_2 array at different current density, 1,500 mA g^{-1} and 3,000 mA g^{-1}, respectively

Besides, carbon layer coated on the nanorods acts as both buffering cushion for the intrinsic large volume change and electrical conducting path. As a result, the capacity retention and cyclability of the electrode have been improved largely. The electrode design approach could be applicable for preparation of other electrode materials.

References

1. W.M. Zhang, J.S. Hu, Y.G. Guo, S.F. Zhang, L.S. Zhang, W.G. Song, L.J. Wan, Adv. Mater. **20**, 1160 (2008)
2. J. Hassoun, G. Derrien, S. Panero, B. Scrosati, Adv. Mater. **20**, 3169 (2008)
3. A.M. Cao, J.S. Hu, H.P. Liang, L.J. Wan, Angew. Chem. Int. Ed. **44**, 4391 (2005)
4. J. Chen, L. Xu, W. Li, X. Gou, Adv. Mater. **17**, 582 (2005)
5. Y.S. Hu, L. Kienle, Y.G. Guo, J. Maier, Adv. Mater. **18**, 1421 (2006)
6. X.W. Lou, Y. Wang, C. Yuan, J.Y. Lee, L.A. Archer, Adv. Mater. **18**, 2325 (2006)
7. G. Derrien, J. Hassoun, S. Panero, B. Scrosati, Adv. Mater. **19**, 2336 (2007)
8. D. Larcher, S. Beattie, M. Morcrette, K. Edström, J.C. Jumas, J.M. Tarascon, J. Mater. Chem. **17**, 3759 (2007)
9. P.G. Bruce, B. Scrosati, J.M. Tarascon, Angew. Chem. Int. Ed. **47**, 2930 (2008)
10. H. Kim, J. Cho, Nano Lett. **8**, 3688 (2008)
11. Y.G. Wang, H.Q. Li, Y.Y. Xia, Adv. Mater. **18**, 2619 (2006)
12. M.H. Park, K. Kim, J. Kim, J. Cho, Adv. Mater. **21**, 1 (2009)
13. Y. Idota, T. Kubota, A. Matsufuji, Y. Maekawa, T. Miyasaka, Science **276**, 1395 (1997)
14. I.A. Courtney, J.R. Dahn, J. Electrochem. Soc. **144**, 2045 (1997)
15. T. Brousse, R. Retoux, U. Herterich, D.M. Schleich, J. Electrochem. Soc. **145**, 1 (1998)
16. M.S. Park, G.X. Wang, Y.M. Kang, D. Wexler, S.X. Dou, H.K. Liu, Angew. Chem. Int. Ed. **46**, 750 (2007)
17. Y. Wang, K. Takahashi, K. Lee, G. Cao, Adv. Funct. Mater. **16**, 1133 (2006)
18. Y. Wang, H.C. Zeng, J.Y. Lee, Adv. Mater. **18**, 645 (2006)
19. D.W. Kim, I.S. Hwang, S.J. Kwon, H.Y. Kang, K.S. Park, Y.J. Choi, K.J. Choi, J.G. Park, Nano Lett. **7**, 3041 (2007)
20. Y. Wang, J.Y. Lee, J. Phys. Chem. B. **108**, 17832 (2004)
21. Z. Ying, Q. Wan, H. Cao, Z.T. Song, S.L. Feng, Appl. Phys. Lett. **87**, 113108 (2005)
22. X.M. Sun, J.F. Liu, Y.D. Li, Chem. Mater. **18**, 3486 (2006)
23. H. Li, Q. Wang, L. Shi, L. Chen, X. Huang, Chem. Mater. **14**, 103 (2002)
24. X.W. Lou, D. Deng, J.Y. Lee, L.A. Archer, Chem. Mater. **20**, 562 (2008)
25. X.M. Sun, Y.D. Li, Angew. Chem. Int. Ed. **43**, 597 (2004)
26. A.C. Ferrari, J. Robertson, Phys. ReV. B. **61**, 14095 (2000)
27. R. Demir Cakan, Y.S. Hu, M. Antonietti, J. Maier, M.M. Titirici, Chem. Mater. **20**, 1227 (2008)